Gas Permeation Properties of Poly(ether imide) Segmented Copolymers

Ken-ichi Okamoto,* Masafumi Fujii, Shuusaku Okamyo, Hajime Suzuki, Kazuhiro Tanaka, and Hidetoshi Kita

Faculty of Engineering, Department of Advanced Materials Science and Engineering, Yamaguchi University, Ube, Yamaguchi 755, Japan

Received March 14, 1995; Revised Manuscript Received June 21, 1995[⊗]

ABSTRACT: Poly(ether imide) segmented copolymers were prepared from polyether−diamine and comonomer diamine with acid anhydride. They have microphase-separated structures consisting of microdomains of rubbery polyether segments and of glassy polyimide segments. The gas permeation occurs through the polyether segment microdomains, and the polyimide segment microdomains contribute to mechanical properties and film-forming ability. The poly(ethylene oxide) (PEO)-based copolymers effect very high CO_2/N_2 separation, for example, permeability coefficient to CO_2 $P_{CO_2} = 1.4 \times 10^{-8}$ cm^3 (STP) cm^2/(cm s cmHg) and permeability ratio of CO_2 over N_2 $P_{CO_2}/P_{N_2} = 70$ at 298 K. This high permselectivity is attributed to high solubility selectivity due to the affinity of CO_2 to PEO segments. On crystallization of PEO segment microdomains, P_{CO_2} decreases but P_{CO_2}/P_{N_2} does not change. The effects of PEO content, PEO block length, kind of acid anhydride and diamine, temperature, and feed pressure on P_{CO_2} and P_{CO_2}/P_{N_2} are investigated.

Introduction

Recovery of CO_2 from flue gas containing 10−20% CO_2 is an important objective in view of the global warming. Membrane separation is one of the potential methods to remove CO_2 from flue gas with reduced energy consumption. Facilitated transports of CO_2 in ion-exchange or liquid membranes have been intensively investigated,[1] because they have high permselectivity due to the chemical interaction between CO_2 and carrier molecules. However, they have not been used because of their characteristic shortcomings. Solid polymeric membranes such as cellulose acetate have been used for CO_2 separation from natural gas, enhanced oil recovery, etc.[2] They have a permeability coefficient to CO_2, P_{CO_2}, of 10 Barrer (1 Barrer = 10^{-10} cm^3 (STP) cm^{-1} s^{-1} cmHg^{-1}) and a permeability ratio of CO_2 over CH_4, P_{CO_2}/P_{CH_4}, of 30−40. Fluorine-containing polyimides have P_{CO_2} of 10−60 Barrer and P_{CO_2}/P_{CH_4} of 40−70.[3−6] However, these polyimides have a low permeability ratio of CO_2 over N_2, $P_{CO_2}/P_{N_2} \sim 20$. For practical application, it is necessary to develop membrane materials having a much higher performance: e.g., $P_{CO_2} > 100$ Barrer and $P_{CO_2}/P_{N_2} > 70$.[7]

We previously reported preliminary results concerning the excellent performance of CO_2/N_2 separation by poly(ether imide) segmented copolymers.[8] This paper describes gas permeation properties of the poly(ether imide) segmented copolymers in detail.

Experimental Section

Bis(3-aminopropyl)poly(ethylene oxide) with an average block length, n, of poly(ethylene oxide) (PEO) of 9 (PEO1), 23 (PEO2), 52 (PEO3), and 201 (PEO4) were supplied from Kawaken Fine Chemicals Co. Ltd. Bis(3-aminopropyl)poly(propylene oxide) with an n of poly(propylene oxide) (PPO) of 33 was supplied from Mitsui Petrochemical Industries Ltd. Bis(3-aminopropyl)polytetrahydrofuran with an n of polytetrahydrofuran (PTHF) of 30 was supplied from BASF Aktiengessellchaft. These polyether diamines were used without further purification. 4,4′-Oxydianiline (ODA), 3,5-diaminobenzoic acid (DABA), 1,3-phenylenediamine (mPD), 4,4′-diaminodiphenyl sulfone (pDDS), 3,3′-diaminodiphenyl sulfone (mDDS), and *p*-aminophenoxy phenyl sulfone (APPS) were used as comonomer diamines. 3,3′,4,4′-Biphenyltetracarboxylic dianhydride (BP), pyromellitic dianhydride (PM), and 4,4′-hexafluoroisopropylidene phthalic anhydride (6F) were used as acid anhydrides. These comonomer diamines and acid anhydrides were commercially available and purified by vacuum sublimation before use.

Polyether-containing copoly(amic acid)s were prepared at a concentration of 10 wt % solids by slow addition of a stoichiometric amount of the acid anhydride to a mechanically stirred *N,N*-dimethylacetamide solution of the polyether diamine and the comonomer diamine(s) under nitrogen at room temperature. The solutions were stirred for 6−12 h. Membranes of the copoly(amic acid)s of 50−170 μm in thickness were prepared by casting solutions onto Teflon Petri dishes and drying at 353 K for 10 h. The membranes were thermally imidized at 443 K for 20 h in vacuo.

Structures of the poly(ether imide) segmented copolymers are shown in Figure 1. The copolymers prepared in this study are listed in Table 1. The figures in parentheses in the copolymer designation refer to the feed weight percentage of the polyether diamine to total diamines. For the copolyimides containing ODA and DABA moieties, the feed weight ratio of ODA to DABA is 4.

Differential scanning calorimetry (DSC) was measured with a Seiko Instruments Inc. DSC-5200 at a heating and cooling rate of 10 K/min. Glass transition temperatures (T_g) and melting temperatures (T_m) were determined from the onset points of the signals on the first heating run. The density was measured by a floating method using xylene−carbon tetrachloride solutions. Wide angle X-ray diffraction (WAXD) was recorded using a Rigakudenki X-ray diffractometer using Cu Kα irradiation.

Dynamic mechanical spectra of the copolymers were measured with a Rheometrics mechanical spectrometer (RSAII) at 1 and 10 Hz from 123 to 623 K and at a peak strain amplitude of 0.20%.

Permeability coefficients P and the diffusion time lag θ were measured by a vacuum time-lag method at 1−10 atm and 273−353 K. The apparent diffusion coefficient D was calculated from $D = l^2/(6\theta)$ where l is the film thickness. The apparent solubility coefficient S was evaluated from $S = P/D$.

Results and Discussion

Characterization Results. The characteristics of the poly(ether imide) segmented copolymers are listed

[⊗] Abstract published in *Advance ACS Abstracts,* August 15, 1995.

0024-9297/95/2228-6950$09.00/0

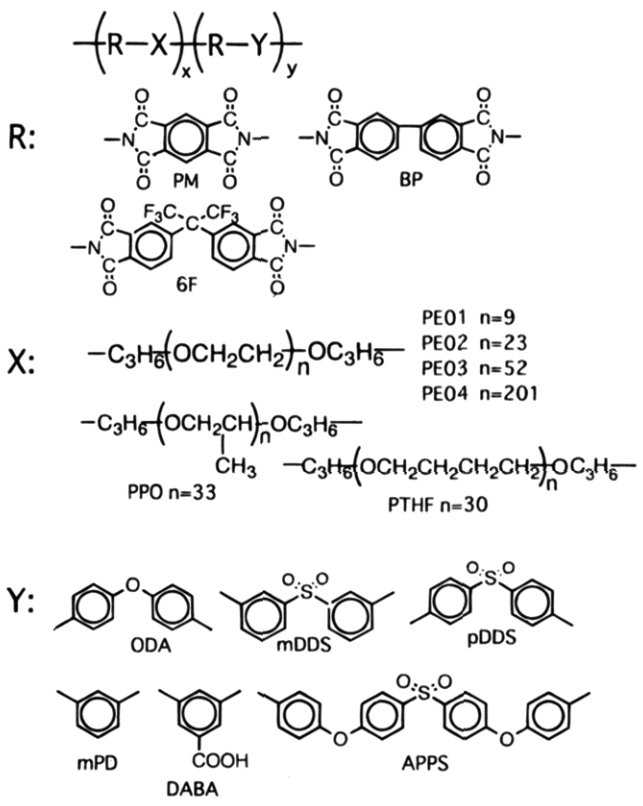

Figure 1. Chemical structures of poly(ether imide) segmented copolymers.

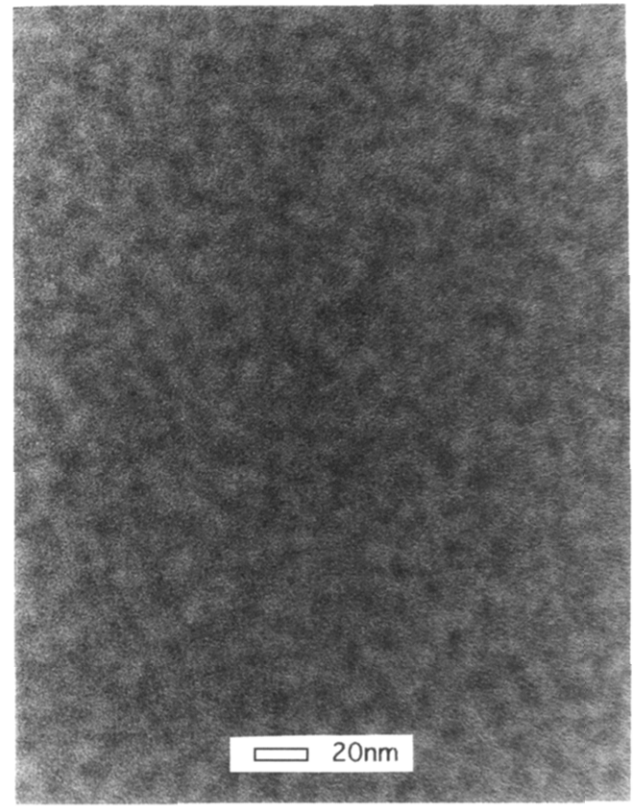

Figure 2. Transmission electron microphotograph of a thin film of BP-PD/PEO4(80).

in Table 1. The copolymers have two glass transition temperatures and one melting temperature. From a comparison of T_g and T_m between the copolymers and the corresponding polyether diamines, the lower glass transition temperature, T_{g_1}, and T_m are attributed to polyether segments of the hydrophilic diamine moieties and the higher glass transition temperature, T_{g_2}, is attributed to polyimide segments of the comonomer diamine moieties. This indicates that the copolymers have microphase-separated structures consisting of microdomains of hydrophilic and rubbery polyether segments and of hydrophobic and glassy polyimide segments. The microphase-separated structure was also demonstrated by transmission electron microscopy (TEM) observation. In Figure 2, the dark areas refer to microdomains of PEO segments stained with RuO_4 vapor,[9] which are rather small and on the order of 10 nm. With an increase in average block length, n, of PEO, T_{g_1} decreases for the PEO-based copolymers, whereas it increases for the PEO diamines. In PEO4 there is no difference in T_{g_1} between the copolymers and the diamine. T_{g_1}'s are higher for the PEO1-based copolymers than for the PEO1 diamine and the PEO4-based copolymers by 43 and 25 K, respectively. This suggests that the segmental motion of PEO in the PEO1-based copolymers is reduced by the glassy polyimide segments.

The polyether content, [PE], refers to the weight percentage of the hydrophilic diamine moieties, namely $-C_3H_6$(polyether block)C_3H_6- chains, which was calculated from the feed monomer composition. The volume percentages of the hydrophilic diamine moieties, which were estimated using the densities of the corresponding polyimides, were larger than the wt % values by 3–4%, e.g., [PE] = 48.8 wt % or 52.6 vol % for BP-ODA/PEO2(75).

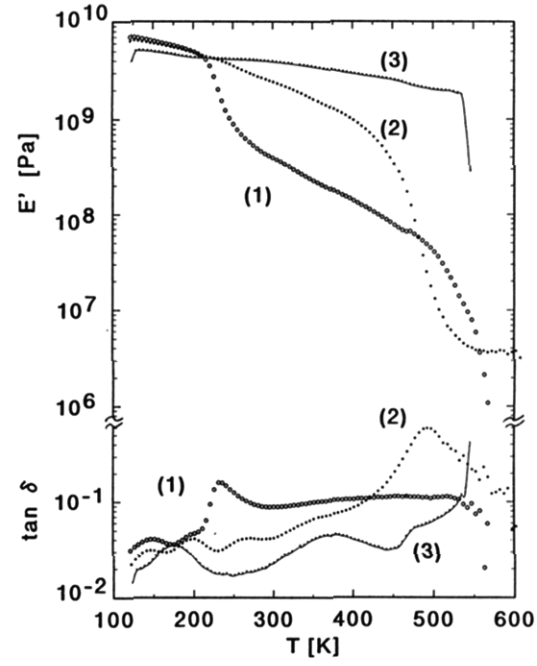

Figure 3. Dynamic mechanical spectra of (1) BP-ODA/DABA/PEO3(75), (2) BP-ODA/DABA/PEO2(50), and (3) BP-ODA.

The poly(ether imide) segmented copolymers form good films and have good mechanical strength. Thin films of the copolymers were easily prepared on glass plates, but could not be taken off the glass plates because of strong adhesion. Therefore, rather thick films were used for the experiments.

Figure 3 shows dynamic mechanical spectra of the copolymers. The modulus E' decreases drastically around T_{g_1} for BP-ODA/DABA/PEO3(75) with [PE] = 51.9 wt %, but not for BP-ODA/DABA/PEO2(50) with

Table 1. Physical Properties of Poly(ether imide) Segmented Copolymers[a]

code	copolymer[b]	[PE] (wt %)	η (dL/g)	density (g/cm^3)	T_{g_1} (K)	T_{g_2} (K)	T_m (K)
B0	BP-ODA	0		1.366		543	
B1	BP-ODA/DABA/PEO1 (75)	41.2	0.59	1.317	237	512	303
B2	BP-mDDS/PEO1(80)	47.4	0.86	1.290			
B3	BP-ODA/DABA/PEO2(50)	27.0	1.15	1.339	231	523	298
B4	BP-ODA/DABA/PEO2(60)	34.6	1.42	1.324	227	517	303
B5	BP-ODA/DABA/PEO2(70)	43.3	2.18	1.318	231	511	301
B6	BP-ODA/DABA/PEO2(80)	53.4	0.68	1.272	229	514	303
B7	BP-ODA/PEO3(75)	52.3	0.89	1.262	217	509	269
B8	BP-ODA/PEO3(80)	58.0	0.70	1.262			
B9	BP-ODA/DABA/PEO3(75)	51.9	0.63	1.274	216	521	298
B10	BP-ODA/DABA/PEO3(80)	57.4	0.84	1.259	217	522	293
B11	BP-mDDS/PEO3(75)	54.7	0.41	1.266			
B12	BP-APPS/PEO3(80)	64.7	0.62	1.227	221	518	294
B13	BP-mPD/PEO4(80)	53.1	2.36	1.292	212	497	297
B14	BP-ODA/PEO4(80)	62.3	1.57	1.253			
BPPO	BP-ODA/DABA/PPO(80)	57.0	0.48	1.139	201	479	ND
BPTHF	BP-ODA/DABA/PTHF(80)	57.6	0.39	1.147	190	550	260
P1	PM-mPD/PEO1(80)	45.9	0.51	1.352	232	ND	297
P2	PM-ODA/DABA/PEO1(80)	51.1	0.50	1.297	238	ND	289
P3	PM-mDDS/PEO1(85)	56.9	0.33	1.300			
P4	PM-ODA/PEO2(75)	53.6	0.29	1.295			
P5	PM-mPD/PEO3(80)	55.9	0.13	1.323	211	ND	268
P6	PM-APPS/PEO3(80)	68.3	0.21	1.253	218	ND	289
P7	PM-APPS/PEO4(70)	61.2	0.62	1.239	207	643	302
P8	PM-mPD/PEO4(80)	58.9	0.30	1.292	212	ND	240
P9	PM-ODA/PEO4(80)	66.6	1.18	1.261	211	ND	297
P10	PM-pDDS/PEO4(80)	68.6	0.41	1.260	211	588	303
F0	6F-ODA	0	2.0	1.432		572	
F1	6F-ODA/PEO3(25)	9.6	1.47	1.426	215	497	306
F2	6F-ODA/PEO3(50)	23.3	1.39	1.406		492	310
F3	6F-ODA/PEO3(80)	50.5	0.46	1.327	219		306
	PEO1 diamine (n = 9)				194		255
	PEO2 diamine (n = 23)				204		301
	PEO3 diamine (n = 52)				207		316
	PEO4 diamine (n = 201)				211		331
	PPO diamine (n = 33)				194		265
	PTHF diamine (n = 30)				190		311

[a] η is inherent viscosity at 0.5 wt % and 298 K of the copoly(amic acid) in DMAc solution. T_{g_1} and T_{g_2} are glass transition temperatures. T_m is the melting temperature. [PE] is the polyether content. [b] The figure in parentheses refers to feed ratio (wt %) of the polyether diamine to total diamines.

Table 2. Modulus E' at 323 K for Poly(ether imide) Segmented Copolymers

code	polyether	[PE] (wt %)	10^{-8} E' (Pa)
B0		0	35
B1	PEO1	41.2	1.6
B3	PEO2	27.0	20
B4	PEO2	34.6	12
B5	PEO2	43.3	4.6
B6	PEO2	52.3	0.31
B9	PEO3	51.9	3.0
P2	PEO1	51.1	0.60

[PE] = 27.0 wt %. Table 2 lists the E' values at 323 K for the copolymers. For a series of the PEO2-based copolymers, the decrease in E' with increasing [PE] is significant above 40 wt % [PE]. These results suggest that the fraction of PEO segment microdomains forming the continuous phase increases significantly with increasing [PE] from 40 to 55 wt %. Also, E' is in the order PEO3 > PEO2 > PEO1 for the copolymers having similar [PE]s.

Permeation Properties. Table 3 lists permeability, diffusivity, and solubility coefficients and ratios of the coefficients for the CO_2/N_2 system in the poly(ether imide) segmented copolymers at 298 K. The PEO-based copolymers have high permeability ratios of CO_2 over N_2 up to 77 at 298 K. This high permselectivity is due to the high solubility selectivity.

For polymeric membranes with a microphase-separated structure, it is important to know how much each phase contributes to the diffusion and sorption. Judging from the data for the polyimides from BP, PM, and 6F,[10,11] the diffusivity coefficients to CO_2 and N_2 will be much larger for the polyether segment microdomains than for the polyimide segment microdomains, whereas the solubility coefficients will be rather smaller for the former. This suggests that the diffusion and therefore the permeation occur through the polyether segment microdomains and the polyimide segment microdomains act as partially immobilizing adsorption sites of the diffusing penetrants. It is well-known that the immobilizing adsorption causes significant increases in the diffusion time lag but has only minor effects on the steady state permeation.[12] In the present study, the D values for the poly(ether imide) segmented copolymers were determined from the time lag values, and S was determined from $S = P/D$. Therefore, it must be checked whether the D and S values determined thus really reflect the diffusion and sorption properties of the PEO segment microdomains. P and θ, and therefore D and S, for CO_2 and N_2 for the PEO-based copolymers (B5, B6, and B7) were found to be independent of feed pressure up to 10 atm. The sorption isotherms of CO_2 in the copolymers (B6 and B7) were measured gravimetrically using a Sartorius microelectrobalance. The sorption equilibrium was attained in a short time less than 10 min. The solubility coefficients S_{e,CO_2} were found to be independent of pressure and nearly equal to the S_{CO_2} listed in Table 3. The S_{e,CO_2} observed for B7, 1.7×10^{-2} cm^3 (STP) cm^{-3} cmHg^{-1}, is much smaller

Table 3. *P*, *D*, and *S* Data for Poly(ether imide) Segmented Copolymers at 298 K and 2 atm[a]

code	copolymer	[PE] (wt %)	P_{CO_2}	P_{CO_2}/P_{N_2}	D_{CO_2}	D_{CO_2}/D_{N_2}	S_{CO_2}	S_{CO_2}/S_{N_2}
B0	BP-ODA	0	0.78		0.09		9.0	
B1	BP-ODA/DABA/PEO1(75)	41.2	1.40	68	0.93	0.79	1.5	86
B2	BP-mDDS/PEO1(80)	47.4	1.72	75	1.32	0.82	1.3	91
B5	BP-ODA/DABA/PEO2(70)	43.3	9.5	70	5.7	0.95	1.7	73
B6	BP-ODA/DABA/PEO2(80)	53.4	24	69	15	0.74	1.6	93
B7	BP-ODA/PEO3(75)	52.3	55	67	31	0.82	1.81	83
B8	BP-ODA/PEO3(80)	58.0	68	65	33	0.82	2.1	79
B10	BP-ODA/DABA/PEO3(80)	57.4	66	69	33	0.92	2.0	77
B11	BP-mDDS/PEO3(75)	54.7	54	70				
B12	BP-APPS/PEO3(80)	64.7	72	70	33	0.89	2.2	79
B13	BP-mPD/PEO4(80)	53.1	65	68	24	0.86	2.7	75
B14	BP-ODA/PEO4(80)	62.3	91	65				
BPO	BP-ODA/DABA/PPO(80)	57.0	119	28	65	0.84	1.85	33
BTH	BP-ODA/DABA/PTHF(80)	57.6	104	29				
P1	PM-mPD/PEO1(80)	45.9	9.5	75	5.3	0.87	1.79	86
P2	PM-ODA/DABA/PEO1(80)	51.1	7.7	77	4.5	0.79	1.71	97
P3	PM-mDDS/PEO1(85)	56.9	6.4	75	3.7	0.68	1.7	114
P4	PM-ODA/PEO2(75)	53.6	28	69	15	0.85	1.9	81
P5	PM-mPD/PEO3(80)	55.9	77	67	34	0.85	2.3	79
P6	PM-APPS/PEO3(80)	68.3	126	65	67	0.68	1.9	97
P7	PM-APPS/PEO4(70)	61.2	103	67	42	0.90	2.5	75
P8	PM-mPD/PEO4(80)	58.9	121	67	58	0.86	2.1	77
P9	PM-ODA/PEO4(80)	66.6	122	70				
P10	PM-pDDS/PEO4(80)	68.6	140	70				
F0	6F-ODA	0	20	25	1.5	1.5	13.0	15
F1	6F-ODA/PEO3(25)	9.6	9.7	33	0.78	1.6	12.5	21
F2	6F-ODA/PEO3(50)	23.3	4.4	44	0.93	1.4	4.7	31
F3	6F-ODA/PEO3(80)	50.5	19.2	65	8.2	1.0	2.4	63

[a] *P*, *D*, and *S* are in Barrer (10^{-10} cm^3 (STP) cm^{-1} s^{-1} cmHg^{-1}), 10^{-8} cm^2 s^{-1} and 10^{-2} cm^3 (STP) cm^{-3} cmHg^{-1}, respectively.

than that estimated from the additivity, 4.4×10^{-2} cm^3 (STP) cm^{-3} cmHg^{-1} and is rather close to the estimated contribution from PEO segment microdomains, 1.3×10^{-2} cm^3 (STP) cm^{-3} cmHg^{-1}. These results indicate that the polyimide segment microdomains make only minor contributions to sorption, diffusion, and permeation of the copolymers. The reason is not clear at present, and further investigation is in progress. It is thus acceptable to adopt *D* and *S* determined from θ for discussion in this study.

Figure 4 shows plots of log *D* versus molecular diameter, *d*, of penetrant gases for BP-ODA/DABA/PEO3(80), poly(dimethylsiloxane) (PDMS), and polyimide (6F-TMPD) prepared from 6F and tetramethyl-*p*-phenylenediamine. For these polymers log *D* is linear in *d*. The molecular-size dependence of *D* for BP-ODA/DABA/PEO3(80) is similar to that for PDMS and smaller than that for 6F-TMPD. The *D* values for BP-ODA/DABA/PEO3(80) are larger than those for 6F-TMPD. 6F-TMPD has been reported to have a larger *D* and a smaller molecular-size dependence of *D* among polyimides because of a less efficient packing of polymer chains.[6] The gas permeation in BP-ODA/DABA/PEO3-(80) is therefore suggested to occur through rubbery PEO segment microdomains.

Figure 5 shows plots of log *S* versus the Lennard-Jones force constant ϵ/k of penetrant gases for BP-ODA/DABA/PEO3(80) together with the data for PDMS and 6F-TMPD. Here log *S* is linear in ϵ/k. The S_{CO_2} for BP-ODA/DABA/PEO3(80) is about 3 times larger than predicted from the correlation line, suggesting an affinity of CO_2 molecules to the polar PEO segments. Although CO_2 is nonpolar, it has a high polarizability and a high quadrupole moment as compared with other gases.[13] This may be the reason for the affinity of CO_2 molecules to the PEO segments.

The PPO- and PTHF-based copolymers have a much lower permselectivity of CO_2 over N_2 as compared with the PEO-based copolymers because of the lower solubility selectivity. This seems due to the fact that PPO and PTHF segments are less hydrophilic than PEO segments.

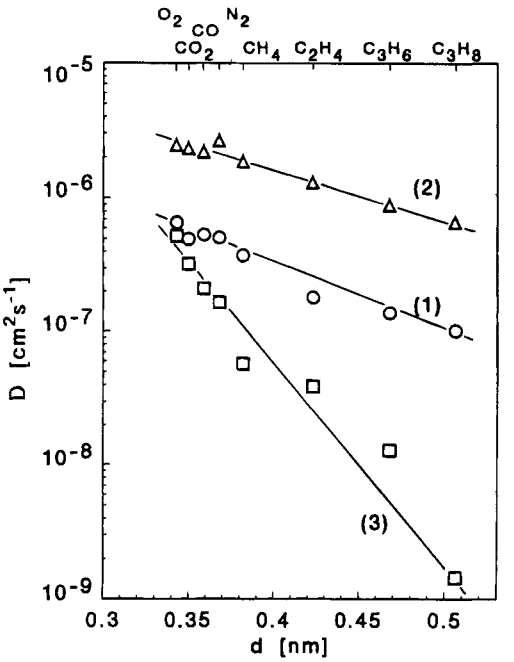

Figure 4. Plots of log *D* versus molecular diameter of penetrant gases for (1) BP-ODA/DABA/PEO3(80), (2) PDMS, and (3) 6F-TMPD at 308 K and 1 atm. The *D* values for 6F-TMPD were determined from $D = P/S$, where *S* values were from the equilibrium sorption measurements. The other values were determined from the diffusion time lags (see text).

The effects of [PE] on P_{CO_2} and P_{CO_2}/P_{N_2} for the PEO-based copolymers at 298 K are shown in Figures 6 and 7, respectively. Above 40 wt % [PE], P_{CO_2} increases significantly with an increase in [PE], except for the PEO1-based copolymers where it is less dependent on [PE]. P_{CO_2} is larger for the copolymers having the longer

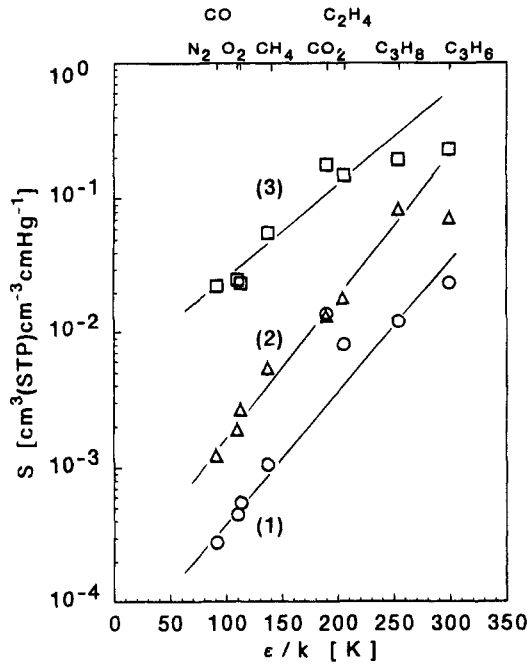

Figure 5. Plots of log S versus the Lennard-Jones force constant of penetrant gases for (1) BP-ODA/DABA/PEO3(80), (2) PDMS, and (3) 6F-TMPD at 308 K and 1 atm. The S values for 6F-TMPD were determined from the equilibrium sorption measurements. The other values were determined from $S = P/D$, where D values were from the diffusion time lags (see text).

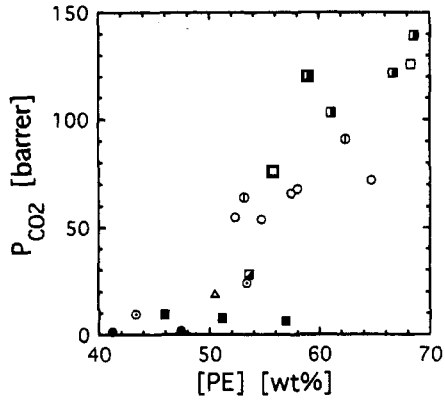

Figure 6. Effects of the content of PEO segment on P_{CO_2} at 298 K for the PEO-based copolymers; BP/PEO1 (●), PM/PEO1 (■), BP/PEO2 (⊙), PM/PEO2 (◪), BP-PEO3 (○), PM-PEO3 (□), 6F/PEO3 (△), BP/PEO4 (◑), and PM/PEO4 (◨).

average block length of PEO, i.e., PEO4 > PEO3 > PEO2 ≫ PEO1. When comparing copolymers with similar [PE]s, P_{CO_2} depends on the kind of acid anhydride, namely, in the order PM > BP > 6F, whereas it depends hardly on comonomer diamine. The variation in P_{CO_2} mentioned above is due mainly to the variation in D_{CO_2}. P_{CO_2}/P_{N_2} depends slightly on the average block length of PEO; i.e., the ratio for PEO1 (75 at 298 K) is a little larger than in PEO2 through PEO4 (65–70 at 298 K). The permeability ratio is independent of [PE] above 43 wt % and the kind of acid anhydride and comonomer diamine. The permeability ratio decreases with a decrease in [PE] below 43 wt %, as can be seen in B1, F1, and F2. These results, in addition to the results of dynamic mechanical properties, indicate that the permeation occurs through microdomains of rubbery PEO segments and the polyimide segments contribute to mechanical properties and film formation. In general, the segmented copolymers with the shorter average

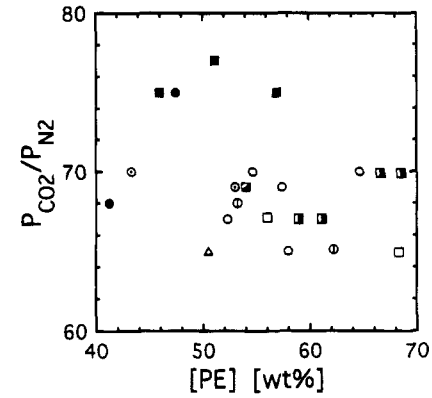

Figure 7. Effects of content of PEO segment on P_{CO_2}/P_{N_2} at 298 K for the PEO-based copolymers. The symbols are the same as in Figure 6.

block length tend to have a less clear phase-separated structure. In the PEO1-based copolymers, because of the very short block length ($n = 9$), the PEO segment microdomains may not be detectable or the intermediate phase between the PEO segment phase and hydrophobic polyimide phase may play a considerable role in the permeation properties. This results in a permeation behavior a little different from that of the other PEO-based copolymers.

Mixed gas permeation experiments were also carried out by a vacuum method followed by gas chromatographic analysis of the permeate. The PEO-based copolymers displayed the similar high performance for a CO_2/N_2 mixture (18 mol % CO_2); e.g., $P_{CO_2} = 75$ and 97 Barrer, $P_{CO_2}/P_{N_2} = 65$ and 49 for PM-mPD/PEO3-(80) at 298 and 308 K, respectively, and 2 atm.

The P, D, and S data mentioned above are for the samples in the amorphous state of polyether segment microdomains. Polyether segment microdomains crystallize gradually by standing for a long time at a lower room temperature. The crystallization was confirmed by appearance of crystalline peaks of WAXD at $2\theta = 19°$ and $2\theta = 23°$ and occurred more easily for the polyimides having longer PEO blocks. After standing for 10 h at 273 K to crystallize the PEO segment domains, the membrane samples were heated slowly and subjected to permeation measurements. Figure 8 shows a typical result of the temperature dependence of P_{CO_2} and P_{CO_2}/P_{N_2}. For PM-ODA/PEO4(80), the permeability increases steeply around 303 K due to the melting of the crystalline PEO segment domains. On cooling, it decreases steeply around 288 K due to the crystallization. The crystallization decreases the permeability but does not change the permselectivity. With an increase in temperature, the permselectivity decreases significantly because of a significant reduction in the solubility selectivity. The activation energies for the permeability and diffusivity coefficients, E_P and E_D, respectively, are listed in Table 4. The E_P values are smaller for CO_2 than for N_2 by the differences in the sorption enthalpies H_S between these gases, because the E_D values are similar. The E_P and E_D are larger for the copolymers having a shorter block length of PEO segment, i.e., PEO1 > PEO2 > PEO3 = PEO4, and are a little larger for BP than for PM copolymers. The E_D values for PEO3- and PEO4-based copolymers are similar to values for polyethylene[14] and polybutadiene[15] (36–39 and 31 kJ/mol, respectively) but are much larger than for PDMS (9–11 kJ/mol).[16] The H_S for the PEO-based copolymers ranges from −14 to −19 kJ/mol for CO_2 and from −1 to +5 kJ/mol for N_2. The H_S values

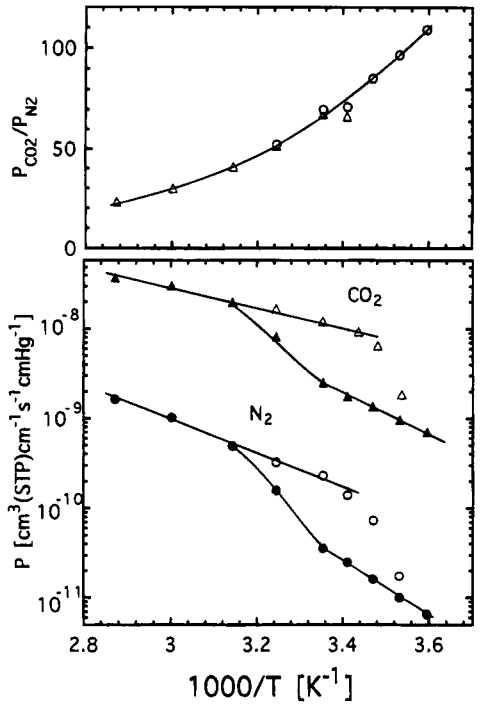

Figure 8. Temperature dependence of P and P_{CO_2}/P_{N_2} for PM-ODA/PEO4(80). For P: (● and ▲) heating run; (○ and △) cooling run. For P ratio: (△) amorphous state of PEO phase; (○) (partially) crystallized state of PEO phase.

Table 4. Activation Energies of P and D for Poly(ether imide) Segmented Copolymers

code	polyether	[PE] (wt %)	E_P (kJ/mol) CO_2	E_P (kJ/mol) N_2	E_D (kJ/mol) CO_2	E_D (kJ/mol) N_2
B1	PEO1	41.2	49	64	65	64
B2	PEO1	47.4	61	80	77	
B5	PEO2	43.3	37	52	52	53
B6	PEO2	53.4	29	46		
B7	PEO3	52.3	24	43	42	42
B11	PEO3	54.7	22	43		
B13	PEO4	53.1	17	35	36	35
B14	PEO4	62.3	19	37		
BPPO	PPO	57.0	18	36	36	36
P3	PEO1	56.9	33	50	49	49
P4	PEO2	53.6	27	46	42	43
P6	PEO3	68.3	18	36	32	31
P7	PEO4	61.2	21	39		
P8	PEO4	58.9	17	37	31	

for CO_2 are a little more negative than for nonpolar rubbery polymers such as polyethylene, polybutadiene, and PDMS (+0.4 or −5.5, −8.8, and −12 kJ/mol, respectively).[14-16]

Figure 9 shows plots of P_{CO_2}/P_{N_2} versus P_{CO_2} at 308 K for the PEO-based copolymers together with data for other polymers. The PEO-based copolymers display about 3 times larger P_{CO_2}/P_{N_2} than other imide and non-imide polymers with a similar P_{CO_2}. Kawakami et al. have reported on the permeabilities to CO_2 and N_2 for PEO/cellulose nitrate (CN) blend films;[17] P_{CO_2} = 8 and 12 Barrer, and P_{CO_2}/P_{N_2} = 38 and 45 at 298 K for the blend films with PEO (M_w = 300) contents of 43 and 50 wt %, respectively. Qipeng et al. have reported on gas permeation of PEO/copolyester−polyurethane (PU) blend films.[18] Compared with the present data, the permeability ratios of CO_2 over N_2 at temperatures below the melting point of PEO were very high; for example, P_{CO_2} = 13 Barrer and P_{CO_2}/P_{N_2} = 150 at 308 K for the PEO/PU blend film with a PEO (M_w = 20 000) content of 30 wt %. This high permselectivity disappears at temperatures above the melting point, i.e., P_{CO_2} = 84 Barrer and P_{CO_2}/P_{N_2} = 25 at 343 K. This is in contrast to the result mentioned above for the poly(ether imide) segmented copolymers where the crystallization of PEO segment domains does not change the permselectivity. These blends do not have the potential for practical applications because of the difficulty of preparing thin membranes from them. The PEO-based copolymers form good films and have a high potential for CO_2/N_2 separation membranes. We have prepared composite membranes composed of a thin layer of BP-ODA/PEO3-(75) and a support layer of polyimide.[19]

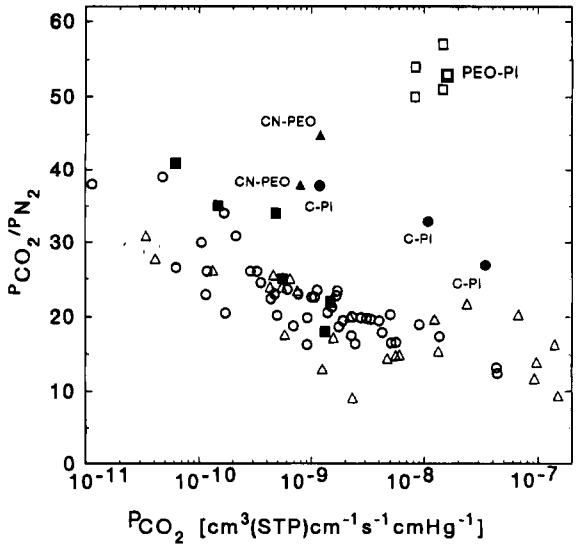

Figure 9. Plots of P_{CO_2}/P_{N_2} versus P_{CO_2} at 308 K for the PEO-based copolymers together with the data for other polymers: (□) poly(ether imide) segmented copolymers; (■) photo-cross-linked BTDA-containing polyimides; (○, ●) other polyimides; (△, ▲) other polymers. C-PI: CARDO-type polyimides. The symbols ● and ▲ are at 298 K.

Conclusions

Poly(ether imide) segmented copolymers have microphase-separated structures consisting of microdomains of rubbery polyether segments and of glassy polyimide segments. The gas permeation occurs through the former domains and the latter domains contribute to both film formation and mechanical properties.

Poly(ethylene oxide) (PEO)-based copolymers display excellent membrane performance for CO_2/N_2 separation; P_{CO_2} = 140 Barrer and P_{CO_2}/P_{N_2} = 70 at 298 K. This permeability ratio is about 3 times larger than for other polymers having a similar P_{CO_2}. This is attributed to the high solubility selectivity due to the affinity of CO_2 to PEO segments.

P_{CO_2} increases with an increasing content and block length of PEO segments, depends on the kind of acid anhydride, and decreases by the crystallization of PEO segment domains. P_{CO_2}/P_{N_2} is almost independent of these variables and decreases with an increase in temperature.

Acknowledgment. The present work was supported partly by a Grant-in-Aid for Developmental Scientific Research (No. 05555212) from the Ministry of Education, Science, and Culture of Japan. The authors also gratefully acknowledge financial support by a research grant from Iketani Science and Technology Foundation (No. 042053B).

References and Notes

(1) LeBlanc, O. H.; Ward, W. J., Jr.; Matson, S. L.; Kimura, S. G. *J. Membr. Sci.* **1980**, *6*, 339. Way, J. D.; Noble, R. D.; Reed, D. L.; Ginley, G. M. *AIChE J.* **1987**, *33*, 480.

(2) Schell, W. J. *J. Membr. Sci.* **1985**, *22*, 218.

(3) Kim, T.-H.; Koros, W. J.; Husk, G. R. *Sep. Sci. Technol.* **1988**, *23*, 1611. Coleman, M. R.; Koros, W. J. *J. Membr. Sci.* **1990**, *50*, 285.

(4) Stern, S. A.; Mi, Y.; Yamamoto, H.; St. Clair, A. K. *J. Polym. Sci., Polym. Phys. Ed.* **1989**, *27*, 1887. Yamamoto, H.; Mi, Y.; Stern, S. A.; St. Clair, K. *J. Polym. Sci., Polym. Phys. Ed.* **1990**, *28*, 2291.

(5) Tanaka, K.; Kita, H.; Okano, M.; Okamoto, K. *Polymer* **1992**, *33*, 585. Tanaka, K.; Okano, M.; Kita, H.; Okamoto, K.; Nishi, S. *Polym. J.* **1994**, *26*, 1186.

(6) Tanaka, K.; Okano, M.; Toshino, H.; Kita, H.; Okamoto, K. *J. Polym. Sci., Polym. Phys. Ed.* **1992**, *30*, 907.

(7) Haraya, K.; Nakaiwa, M.; Itoh, N.; Kamisawa, C. *Kagaku Kogaku Ronbunshu* **1993**, *19*, 714.

(8) Okamoto, K.; Umeo, N.; Okamyo, S.; Tanaka, K.; Kita, H. *Chem. Lett.* **1993**, 225.

(9) Trent, J. S.; Scheinbeim, J. I.; Couchman, P. R. *Macromolecules* **1983**, *16*, 589.

(10) Okamoto, K.; Tanaka, K.; Kit, H. *J. Polym. Sci., Polym. Phys. Ed.* **1989**, *27*, 2621.

(11) Tanaka, K.; Kita, H.; Okamoto, K. *J. Polym. Sci., Polym. Phys. Ed.* **1993**, *31*, 1127.

(12) Paul, D. R.; Kemp, D. R. *J. Polym. Sci., Symp.* **1973**, No. 41, 79. Paul, D. R.; Koros, W. J. *J. Polym. Sci., Polym. Phys. Ed.* **1976**, *14*, 675.

(13) Stogryn, D. E.; Strogryn, A. P. *Mol. Phys.* **1966**, *11*, 371.

(14) Michaels, A. S.; Bixler, H. J. *J. Polym. Sci.* **1960**, *50*, 413.

(15) Amerongen, G. J. *J. Polym. Sci.* **1950**, *5*, 307.

(16) Stern, S. A.; Shah, V. M.; Haedy, B. J. *J. Polym. Sci., Polym. Phys. Ed.* **1987**, *25*, 1263. Venkataraman, K.; Stern, S. A.; Mark, J. E. Annual Report for Gas Research Institute: Investigation of structure-permeability relationships of silicone polymer membranes, Oct 1984–Sept 1985.

(17) Kawakami, M.; Iwanaga, H.; Hara, Y.; Iwamoto, M.; Kagawa, S. *J. Appl. Polym. Sci.* **1982**, *27*, 2387.

(18) Qipeng, G.; Hechang, X.; Dezhu, M. *J. Appl. Polym. Sci.* **1990**, *39*, 2321.

(19) Okamoto, K. Manuscript to be published.

MA950328Q